Journal of Rock Mechanics and Geotechnical Engineering 15 (2023) 1263–1273

Contents lists available at ScienceDirect

Journal of Rock Mechanics and Geotechnical Engineering

journal homepage: www.jrmge.cn

Full Length Article

Analysis of a landfill cover without geomembrane using varied particle sizes of recycled concrete

Charles Wang Wai Ng [a], Cheuk Lam Ng [a], Junjun Ni [b,*], Haowen Guo [a], Qi Zhang [a], Qiang Xue [c], Rui Chen [d]

[a] Department of Civil and Environmental Engineering, Hong Kong University of Science and Technology, Hong Kong, China
[b] School of Transportation, Southeast University, Nanjing, China
[c] State Key Laboratory of Geomechanics and Geotechnical Engineering, Institute of Rock and Soil Mechanics, Chinese Academy of Sciences, Wuhan, 430071, China
[d] Department of Civil and Environmental Engineering, Shenzhen Graduate School, Harbin Institute of Technology, Shenzhen, China

ARTICLE INFO

Article history:
Received 11 April 2022
Received in revised form
2 August 2022
Accepted 15 September 2022
Available online 4 October 2022

Keywords:
Capillary barrier
Landfill cover
Particle size
Recycled concrete

ABSTRACT

Previous studies have demonstrated the effectiveness of a novel three-layer landfill cover system constructed with recycled concrete aggregates (RCAs) without geomembrane in both laboratory and field. However, no systematic investigation has been carried out to optimize the combination of the particle sizes for fine-grained RCAs (FRC) and coarse-grained RCAs (CRC) that can be used for the three-layer landfill cover system. The aim of this paper is to assist engineers in designing the three-layer landfill cover system under a rainfall of 100-year return period in humid climate conditions using an easily controlled soil parameter D_{10} of RCAs. The numerical study reveals that when D_{10} of FRC increases from 0.05 mm to 0.16 mm, its saturated permeability increases by 10 times. As a result, a larger amount of rainwater infiltrates into the cover system, causing a higher lateral diversion in both the top FRC and middle CRC layers. No further changes in the lateral diversion are observed when the D_{10} value of FRC is larger than 0.16 mm. Both the particle sizes of FRC and CRC layers are shown to have a minor influence on the percolation under the extreme rainfall event. This implies that the selection of particle sizes for the FRC and CRC layers can be based on the availability of materials. Although it is well known that the bottom layer of the cover system should be constructed with very fine-grained soils if possible, this study provides an upper limit to the particle size that can be used in the bottom layer (D_{10} not larger than 0.02 mm). With this limit, the three-layer system can still minimize the water percolation to meet the design criterion (30 mm/yr) even under a 100-year return period of rainfall in humid climates.

1. Introduction

The rapid development of urban cities causes an increasing generation of municipal solid waste. Due to its simplicity and cost-efficiency, landfilling is one of the most common ways to manage municipal waste (Wong et al., 2013). A final cover system is a necessary component for a landfill to minimize the generation of leachate and hence to prevent the contamination of ground water. In conventional designs, low permeability materials, including compacted clay and geomembranes, are usually selected for constructing the final landfill cover. However, their performance is often compromised due to desiccation cracking, instability failures and puncture failures (Albright et al., 2006; Amaya et al., 2006; Fox et al., 2014). Therefore, the use of alternative covers has become a hot research topic in recent decades (Zhang and Sun, 2014).

A cover with capillary barrier effects (CCBE) has served as one of the alternatives (Ross, 1990). In general, a typical CCBE consists of two soil layers: a fine-grained soil layer overlying a coarse-grained soil layer. Such layout can inhibit the downward migration of water by utilizing the contrasting permeability of the two soil layers at high suction conditions. Nevertheless, the application of CCBE under humid climates is not recommended (Khire et al., 2000; Albright et al., 2004). This is because under heavy rainfall, water can break through the cover system, and the capillary barrier will not be effective at all. To ensure the effectiveness of a CCBE under humid climates, Ng et al. (2016) proposed a new alternative three-

* Corresponding author.
E-mail addresses: nijunjun@seu.edu.cn, jniaa@connect.ust.hk (J. Ni).
Peer review under responsibility of Institute of Rock and Soil Mechanics, Chinese Academy of Sciences.

https://doi.org/10.1016/j.jrmge.2022.09.004

layer landfill cover system, which is applicable under all-weather conditions. The design introduced an additional compacted layer with low permeability beneath a conventional two-layer CCBE. In this design, the upper CCBE in the three-layer landfill cover system can store and divert rainwater in the overlying fine-grained layer under small rainfall events in arid and semi-arid regions. This is because the unsaturated water permeability of the underlying coarse-grained layer is much smaller than that of the overlying fine-grained layer under such condition. However, when the water permeability of the coarse-grained layer becomes larger than that of the fine-grained layer due to heavy rainfalls in humid regions, water breakthrough occurs at the interface and the additional layer at the bottom can effectively minimize water percolation due to its low permeability. The infiltrated water is thus diverted through the middle coarse-grained layer (Ng et al., 2019a). Since relatively coarse materials (e.g. sand and gravel) are used in the top and middle layers of the cover system, desiccation cracking would not occur in these layers. Also, the low water permeability of the top two layers under high suction conditions can minimize the upward flow of water during evaporation. This protects the bottom fine-grained layer from desaturation and hence the formation of desiccation cracks (Ng et al., 2016).

The working principle of this new landfill cover design is fundamentally different from those of the conventional hydraulic barrier cover system (USEPA, 1993; Qian et al., 2001). This is because the upper two soil layers in the new cover system work as a CCBE and no geomembrane is needed in the new cover system even under the extreme rainfall of humid climates, which is verified by theoretical, experimental studies (Ng et al., 2015b, 2016) and field trial (Ng et al., 2019a, 2022a). In comparison, the top and middle layers of the conventional hydraulic barrier cover system only function as a vegetation supporting layer and a drainage layer, respectively. Geomembrane is therefore required to install above the compacted clay layer in the conventional cover system to minimize percolation under extreme rainfall events (Qian et al., 2001). The alternative all-weather three-layer landfill cover system proposed by Ng et al. (2016) can be used not only in arid and semi-arid regions with low rainfalls, but also in humid regions with extreme rainfalls (Ng et al., 2015a, b, 2016; Chen et al., 2019). Although the alternative cover system proposed by Ng et al. (2016) has been validated under both laboratory and field conditions (Ng et al., 2015a, b, 2016; Chen et al., 2019), no systematic investigation has been carried out for engineers to optimize the combination of particle sizes for fine- and coarse-grained materials that can be used for their design of a three-layer landfill cover system.

Furthermore, sustainable development has attracted increasing attention over the past years. To promote environmental sustainability, the use of recycled concrete aggregates (RCAs) in building and geotechnical applications is common around the world. For example, RCAs can be used for casting new concrete (Oikonomou, 2005; Tabsh and Abdelfatah, 2009; Evangelista and Brito, 2010) or as a pavement material (Gabr and Cameron, 2012; Nwakaire et al., 2020). Since RCAs possess similar hydraulic properties as natural aggregates (Rahardjo et al., 2013a), the use of RCAs as a substitution material for landfill covers is also a possible option. For example, Rahardjo et al. (2013b) replaced the underlying coarse-grained layer of a capillary barrier system using RCAs while maintaining the overall effectiveness of the cover. Similarly, investigations have also been carried out to evaluate the performance of the three-layer landfill cover using RCAs (Ng et al., 2019a, b). In the experiments, Ng et al. (2019a) replaced the middle layer with coarse recycled concrete aggregate (CRC), whereas Ng et al. (2019b) replaced the top and middle layers with fine recycled concrete aggregate (FRC) and CRC. The results showed that the percolation was below the recommended criterion of 30 mm/yr suggested by USEPA (1993). In addition, the typical price for crushing recycled concrete in China is about 20 RMB/t, irrespective of the final size of crushed particles. The unit material price for constructing a three-layer landfill cover system with a given thickness of 0.9 m using RCA is less than 30 RMB/m^2, which is far less than that of the cover system using geomembrane (more than 300 RMB/m^2). These demonstrate the feasibility and practicality of the cover system constructed with RCA under humid climates. It is noted that plants cannot grow properly in alkaline concrete materials. This is because the most suitable soil for plant growth should be slightly acidic. For this reason, biochar, fly ash and slag can be used as potential amendments to improve plant growth under alkaline condition (GarciaCalvo and Hidalgo, 2010; Artiola et al., 2012; Lee and Yang, 2016; Zhao et al., 2019). According to the study by Ng et al. (2019a) and Li et al. (2021), the root depth of grass species (i.e. *Cynodon dactylon* or Vetiver grass) in the capillary barrier system was about 0.3–0.4 m, which is far less than the thickness of the three-layer cover system in this study (0.9 m). Moreover, a geotextile is normally placed between the top fine- and coarse-layers to minimize the fines migration into the coarse layer. The geotextile may also reduce the penetration of roots into the deeper layers (Dobson and Moffat, 1995). Further study is required to study the effectiveness of the three-layer system if plant roots grow through the cover.

Currently, existing studies suggested that the minimum ratio between the water-entry value of FRC layer and CRC layer should be 10, and the water-entry value of CRC should be smaller than 1 kPa (Rahardjo et al., 2007). However, these criteria cannot provide an optimum combination regarding the particle size of RCAs. Theoretically, the capillary diversion can be maximized when the underlying material is infinitely coarser than the overlying fine material (Smesrud and Selker, 2001) and the water-entry value of the coarse material should be close to zero. Due to practical limitations, the selection of appropriate particle size is often based on the availability of materials. Even though the theoretical capillary diversion under a given particle size combination can be calculated by the analytical equation proposed by Smesrud and Selker (2001), the optimum particle sizes corresponding to the maximum lateral diversion are unknown. In order to provide a scientific design guideline for practical applications, the effects of particle size selection of RCAs on the performance of the cover system should be investigated.

This paper aims to assist engineers in designing the three-layer landfill cover system for humid climate conditions using an easily controlled soil parameter D_{10} of RCA. The influence of particle size of RCAs in all layers on the hydrological performance of the three-layer landfill cover system is investigated. First, a two-dimensional (2D) numerical model is validated against the flume test results reported by Lu (2019). Then, a series of parametric study is carried out to investigate the influence of particle sizes of RCAs in all three layers on the pore-water pressure distribution and water balance of the cover system. Finally, practical optimized particle sizes for the three-layer landfill cover system under humid climate conditions are suggested for engineers.

2. 2D finite element analysis

A numerical study is conducted using the 2D finite element software, SEEP/W (2018), to simulate water infiltration into the three-layer landfill cover system. The governing equation for transient seepage analysis in unsaturated soil (Ng and Menzies, 2007; Yao et al., 2021; Ng et al., 2022b) can be expressed by the following equation:

$$\frac{\partial}{\partial x}\left(k_x\frac{\partial H}{\partial x}\right)+\frac{\partial}{\partial y}\left(k_y\frac{\partial H}{\partial y}\right)+Q=m_w\gamma_w\frac{\partial H}{\partial t} \quad (1)$$

where H is the total head, k_x is the water permeability function in the x-direction, k_y is the water permeability function in the y-direction, Q is the applied boundary flux, m_w is the specific moisture capacity, and γ_w is the unit weight of water.

Overall, there are two stages in the numerical simulation. The first stage is to validate the numerical model against the experimental results reported by Lu (2019). The purpose of model validation is to check the reliability of the adopted numerical model (e.g. mesh configuration, boundary conditions and hydraulic properties of materials) by comparing the numerical simulation and experimental results. At the second stage, the validated numerical model is used to investigate the influence of particle size on the performance of a three-layer landfill cover system constructed with RCAs under a 100-year return period of rainfall.

2.1. Analysis plan and input parameters

2.1.1. Model validation

In this study, the numerical model is validated against the 2D flume results from Lu (2019). According to the laboratory test reported by Lu (2019), a three-layer landfill cover was constructed in a 2D flume model, which was 3 m (length) × 1 m (width) × 1.5 m (height) in dimension (Fig. 1). The cover consists of a 0.4 m thick FRC layer on the top, a 0.2 m thick CRC layer in the middle and a 0.3 m thick clayey silt (CS) layer at the bottom. No geomembrane was employed in the cover system. The concrete aggregates used in the study were obtained from a demolition site in Longgang district, Shenzhen, whereas the CS was obtained from an excavation site near the Xiaping landfill cover in Shenzhen. The obtained concrete aggregates were then crushed and sieved to obtain the FRC and CRC used in the experiment. Based on the unified soil classification system (USCS) (ASTM, 2011), the FRC and CRC are classified as well-graded sand (SW) and poorly graded gravel (GP), respectively. The particle size distributions of materials are shown in Fig. 2. To construct the cover system, a 0.05 m thick gravel layer was first placed at the bottom of the flume model to simulate the gas collection layer. The cover materials were then compacted with each spanning a height of 0.02 m, using a 0.2 m × 0.2 m vibrator plate. Geotextiles were inserted between the layer interfaces and the cover surface to prevent particle migrations and surface erosion, respectively. After compaction, the flume model box was inclined. As recommended by the design guideline (GB 51220–2017, 2017), the typical range for the inclination angle of landfill cover systems in China is from 5° to 18°. Therefore, the inclination angle of the flume model was set at 3°, which is close to the lowest value recommended by GB 51220–2017 (2017). By adopting this small inclination angle, there will be no ponding on the top but producing sufficient conservative results.

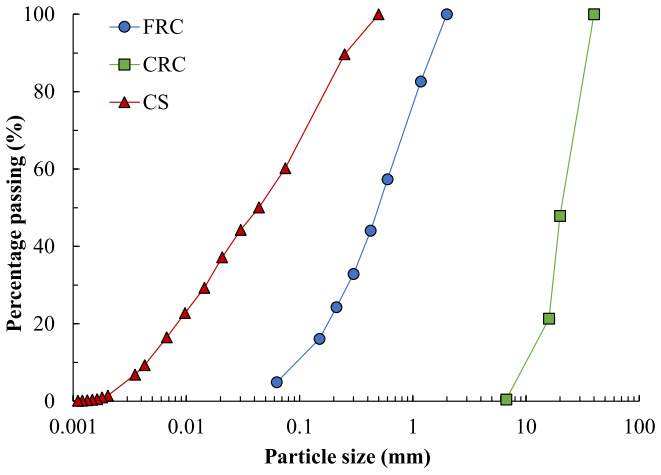

Fig. 2. Particle size distributions of materials used in the three-layer cover system (Lu, 2019).

For the instrumentation, tensiometers and frequency domain reflectometry sensors were installed in the upper (0.75 m), middle (1.5 m) and lower (2.25 m) cross-sections of the flume model to measure pore-water pressure and volumetric water content at depths of 0.1 m, 0.3 m, 0.5 m, 0.7 m and 0.8 m, respectively. In total, nine drain gauges were also installed to measure the infiltration

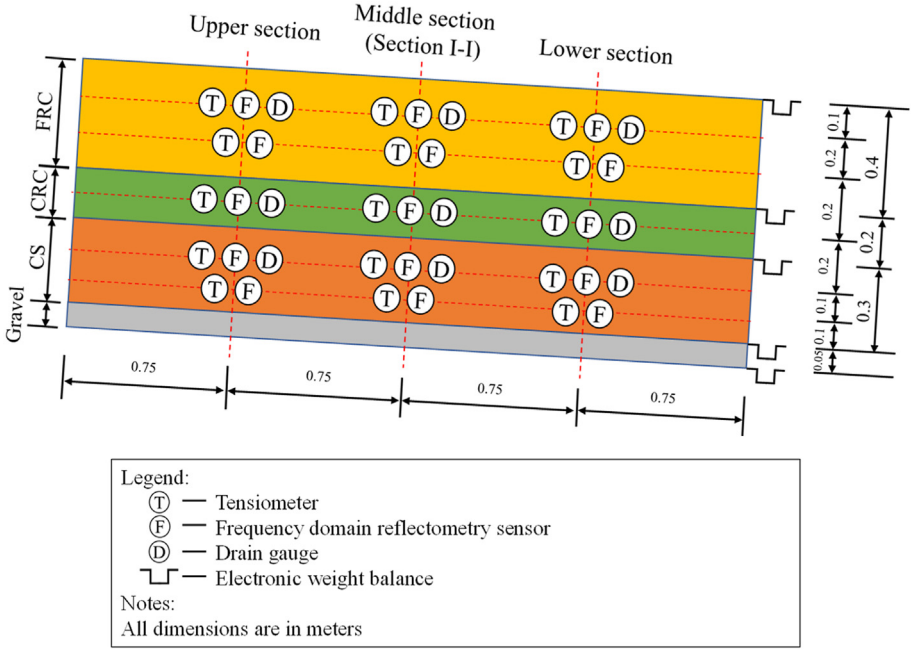

Fig. 1. Layout of instrumentation in the laboratory test.

rate in each layer. A number of holes were drilled on the downstream sidewall of the flume model for collecting the surface runoff, lateral diversion at each soil layer and percolation from the cover system for analysis. As Ng and Pang (2000) demonstrated that the changes in the hysteresis loop of soil become minor after three wetting and drying cycles, the cover system had undergone three wetting and drying cycles to simulate the field condition. Afterwards, the cover system was subjected to a rainfall with an intensity of 36.5 mm/h until saturation, followed by a 120-h drying. During the water infiltration test, a heavy rainfall event with the same intensity of 36.5 mm/h was first applied to the cover system for 12 h. Subsequently, the cover system was allowed to dry under natural condition.

Fig. 3 shows the model geometry and finite element mesh used in SEEP/W (2018). Previous studies revealed that mesh size plays a key role in convergence (Ju and Kung, 1997) and affects the accuracy of transient seepage analysis in unsaturated soil (Vogel and Ippisch, 2008; Vereecken et al., 2016). To ensure the accuracy of rainfall infiltration analysis, the critical mesh size depends on the minimum water diffusion coefficient, D_0, and saturated permeability, k_s (Li et al., 2022). In this study, the minimum water diffusion coefficient is estimated to be 3.07×10^{-7} m^2/s, given that the initial pore water pressure near the soil surface is 18 kPa. The maximum infiltration rate is taken as rainfall intensity, which is 1.7×10^{-6} m/s. Thus, the critical mesh size is estimated as 0.079 m. Considering both numerical accuracy and efficiency, the finite-element discretization in this study is set ranging from 0.025 m to 0.05 m. In total, 3100 rectangular elements are generated in the mesh configuration to simulate the three-layer cover system.

In order to conduct the seepage analysis, the hydraulic properties, including the water retention curves (WRCs) and unsaturated permeability functions, of the used materials are required. All samples were prepared at the degree of compaction of 95% for testing. For simplicity, only the drying WRCs of the materials are considered in this study. Measurements of the WRCs of FRC and CS were performed using a modified pressure plate apparatus (Ng and Pang, 2000). A hanging column apparatus was used to measure the WRC of CRC in accordance with the ASTM D6836-16 (2016) standard. In general, both the van Genuchten (1980) equation and Fredlund and Xing (1994) equation can fit the measured WRC data reasonably well (Leong and Rahardjo, 1997). However, the correction factor in Fredlund and Xing (1994), which forces the volumetric water content to be zero at high suction, does not have a theoretical basis. Hence, the van Genuchten (1980) equation was adopted for fitting the measured data in this study. The equation is expressed as

$$\theta_w = \theta_r + \frac{\theta_s - \theta_r}{\left[1 + (\alpha\psi)^n\right]^m} \tag{2}$$

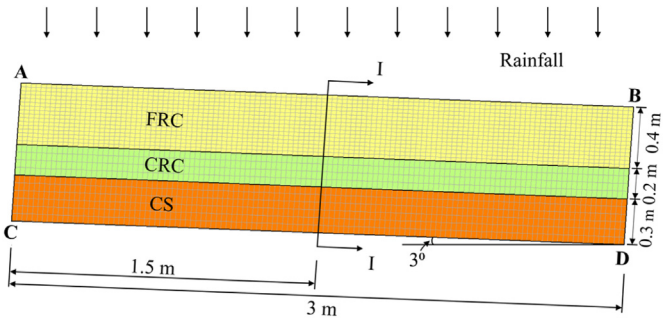

Fig. 3. Finite element mesh used in the seepage analysis.

where θ_w is the volumetric water content at any matric suction ψ ($\psi = -h\gamma_w$, where h is the water pressure head and γ_w is the unit weight of water); θ_s is the saturated water content; θ_r is the residual water content; and α, n and m are the fitting parameters. Fig. 4 presents the measured and fitted WRCs of FRC, CRC and CS. The corresponding fitting parameters are summarized in Table 1. Fig. 5 shows the unsaturated permeability functions of FRC, CRC and CS. They are calculated based on the WRCs shown in Fig. 4 using the van Genuchten-Mualem equation (Mualem, 1976; van Genuchten, 1980). The equation is expressed as

$$k = k_s \frac{\left\{1 - (\alpha\psi)^{n-1}\left[1 + (\alpha\psi)^n\right]^{-m}\right\}^2}{\left[1 + (\alpha\psi)^n\right]^{m/2}} \tag{3}$$

where k is the unsaturated coefficient of permeability at any matric suction ψ. The k_s values of FRC and CS were tested using the flexible wall permeameter according to the ASTM D5084-10 (2010) standard, while constant head method was used for the measurement of CRC as described in ASTM D2434-68 (2006) standard. In summary, the input k_s values for FRC, CRC and CS for the validation run are measured to be 1.7×10^{-6} m/s, 2.5×10^{-1} m/s and 1.7×10^{-8} m/s, respectively. Since k_s is mainly controlled by micropores in soil (Marshall, 1958; Chapuis and Aubertin, 2003), the finer portion of the particle size distribution (such as D_{10} or D_{30}) contributes more to the magnitude of k_s. For simplicity, the widely adopted Hazen (1911) equation (Agus et al., 2005; Bardet et al., 2014) is used to estimate the k_s of cover materials using D_{10} in the parametric study. Given that this study focuses on the variation of k_s of the materials, D_{10} is therefore chosen as the main parameter for numerical analyses. Another advantage of using D_{10} to characterize the cover materials is that engineers can readily and easily conduct their preliminary design analyses in a relatively simple but reasonable manner. It should be noted that D_{10} cannot capture the variations of micropore structure in soils. If the change of soil water retention characteristics (i.e. air entry value and desorption rate) needs to be considered, a full description of the particle size distribution (Fredlund et al., 2000) should be included. The Hazen (1911) equation can be written as

$$k_s = CD_{10}^2 \tag{4}$$

where C is an empirical coefficient, and D_{10} is the effective particle size (cm). In this study, the empirical coefficients were calculated

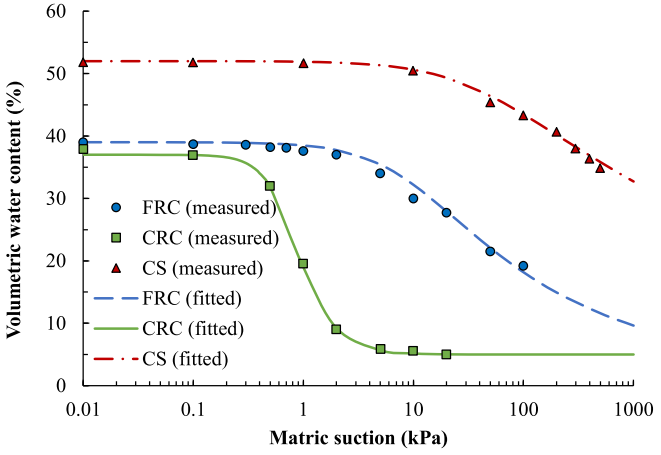

Fig. 4. Measured and fitted WRCs of FRC, CRC and CS.

Table 1
Van Genuchten (1980) fitting parameters for the recycled concrete aggregates and soil.

Parameter	Symbol	Value		
		FRC	CRC	CS
Saturated volumetric water content	θ_S	0.39	0.37	0.52
Residual volumetric water content	θ_R	0.02	0.05	0.01
Van Genuchten (1980) fitting parameters	α (kPa^{-1})	0.12	1.35	0.03
	m	0.25	0.67	0.12
	n	1.33	3.01	1.14

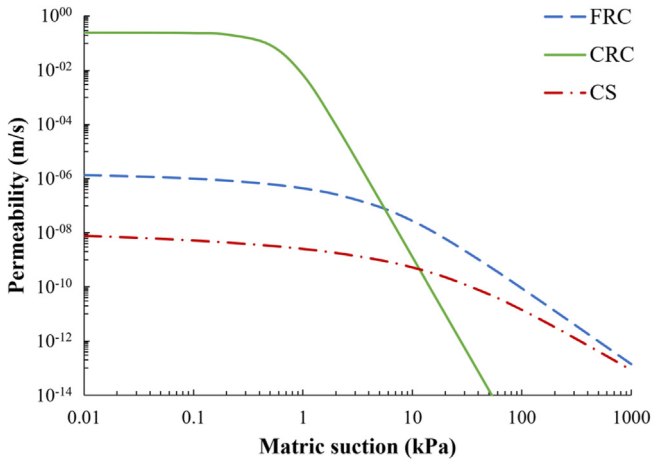

Fig. 5. Permeability functions of FRC, CRC and CS.

based on the k_s and D_{10} values of the materials in the validation run using the Hazen (1911) equation. The D_{10} values for FRC, CRC and CS in the validation run are 0.05 mm, 10.7 mm and 0.002 mm, respectively. The results are summarized in Table 2. The empirical coefficient C values for FRC, CRC and CS are determined to be 7, 22 and 42, respectively. It should be noted that the Hazen (1911) equation using D_{10} is only applicable for predicting the k_s of coarse-grained soil at a loose state (Chapuis, 2012). Thus, the predicted k_s of the compacted cover materials in this study may be overestimated, resulting in a more conservative evaluation of cover performance and design recommendations. Further analyses using more accurate predicting models, i.e. Kozeny-Carman equation (Taylor, 1948; Chapuis, 2004; Sezer et al., 2009), may be necessary to form an improved design guideline in future. Moreover, when studying the mechanical behavior of FRC & CRC and its application in slope stability, some numerical tools, such as Discrete Element Method (DEM), can be adopted. The details of DEM can be found in Cui et al. (2022), Fang et al. (2022) and Yao et al. (2022).

2.1.2. Parametric study

After validating the numerical model, three series of parametric analyses are carried out to investigate the influence of particle size of RCAs on the performance of the cover system. D_{10} is selected to characterize the particle size of the cover materials due to its close correlation with k_s. All the k_s values in the parametric study are calculated based on Hazen's equation in Eq. (4). The first series focuses on the effects of particle size of the FRC layer. Four different D_{10} values of FRC (i.e. 0.05 mm (F0.05), 0.16 mm (F0.16), 0.5 mm (F0.5) and 1.6 mm (F1.6)) are selected. They correspond to the k_s values of 1.7×10^{-6} m/s, 1.7×10^{-5} m/s, 1.7×10^{-4} m/s and 1.7×10^{-3} m/s, respectively. The second series aims to study the influence of D_{10} of CRC layer on the water balance components in the three-layer landfill cover system. Two D_{10} values (10.7 mm (C10.7) and 3.4 mm (C3.4)) are used and they correspond to the k_s values of CRC of 2.5×10^{-1} m/s and 2.5×10^{-2} m/s, respectively. Furthermore, the third series focuses on the particle size of the bottom CS layer. By varying the particle size of CS, the maximum allowable particle size can be determined if the percolation meets the design criterion. Three D_{10} values of CS (i.e. 0.002 mm (CS0.002), 0.006 mm (CS0.006) and 0.02 mm (CS0.02)) are considered. The selected particle sizes correspond to k_s of three different orders of magnitude, ranging from 10^{-8} m/s to 10^{-6} m/s. The D_{10} and the corresponding k_s values of FRC, CRC and CS in the parametric study are summarized in Table 2. Since the water retention capacity of the materials increases with a decreasing D_{10} value, a series of numerical runs was carried out to investigate the influence of WRC on water infiltration in three-layer cover system under a 100-year return period of rainfall with an intensity of 36.8 mm/h (1.02×10^{-5} m/s) for 12 h. By comparing the cases with and without considering the particle size effects on WRC, the differences in surface runoff, lateral diversion and percolation at the end of the 24-h simulation were all less than 2%. Hence, the influence of particle size induced changes in WRC on the water balance results was ignored under the 100-year return period rainfall in this study. This implies that the variation in D_{10} only affects the permeability functions by changing k_s.

Table 2
Summary of numerical analyses in SEEP/W (2018).

Series	ID	k_s of FRC (m/s)	D_{10} of FRC (mm)	k_s of CRC (m/s)	D_{10} of CRC (mm)	k_s of CS (m/s)	D_{10} of CS (mm)	Remark
0	Va	1.7×10^{-6}	0.05	2.5×10^{-1}	10.7	1.7×10^{-8}	0.002	Validation
1	F0.05	1.7×10^{-6}	0.05	2.5×10^{-1}	10.7	1.7×10^{-8}	0.002	Effects of particle size of FRC
	F0.16	1.7×10^{-5}	0.16					
	F0.5	1.7×10^{-4}	0.5					
	F1.6	1.7×10^{-3}	1.6					
2	F0.05C10.7	1.7×10^{-6}	0.05	2.5×10^{-1}	10.7	1.7×10^{-8}	0.002	Effects of particle size of CRC
	F0.05C3.4			2.5×10^{-2}	3.4			
	F0.16C10.7	1.7×10^{-5}	0.16	2.5×10^{-1}	10.7			
	F0.16C3.4			2.5×10^{-2}	3.4			
	F0.5C10.7	1.7×10^{-4}	0.5	2.5×10^{-1}	10.7			
	F0.5C3.4			2.5×10^{-2}	3.4			
	F1.6C10.7	1.7×10^{-3}	1.6	2.5×10^{-1}	10.7			
	F1.6C3.4			2.5×10^{-2}	3.4			
3	CS0.002	1.7×10^{-3}	1.6	2.5×10^{-1}	10.7	1.7×10^{-8}	0.002	Effects of particle size of CS
	CS0.006					1.7×10^{-7}	0.006	
	CS0.02					1.7×10^{-6}	0.02	

Note: Va denotes validation, F denotes FRC in the top layer, C denotes CRC in the middle layer, and CS denotes CS in the bottom layer.

2.2. Numerical procedures

Steady-state seepage analysis is first conducted, to establish the initial pore-water pressure distribution for the following transient seepage analysis in both validation and parametric study. A very small rainfall with an intensity of 0.01 mm/d (1.16×10^{-10} m/s) is applied to the top boundary AB in Fig. 2. The hydraulic head of the bottom boundary CD is set to be −0.2 m, so that the computed PWP at the bottom of the cover is reasonably close to the measured value in the flume test. The left boundary AC and the right boundary BD are set as a zero-flux boundary and a potential seepage face, respectively.

After the steady-state seepage analysis, a transient state analysis was conducted to simulate the drying stage experienced by the flume model prior to the rainfall event as in the flume test (Lu, 2019). An evaporative flux of 3.3×10^{-8} m/s is specified at the top boundary AB for 3.5 d to simulate the drying process (Ng et al., 2015b). Since a gas collection layer is located underneath the three-layer cover system in the physical flume model (Lu, 2019), a potential seepage face is therefore specified at the bottom boundary CD in the drying stage before rainfall. No changes were made to the boundary conditions at AC and BD. Following the end of the drying stage, a rainfall event with an intensity of 36.8 mm/h (1.02×10^{-5} m/s) is applied to the top boundary AB for 12 h. This corresponds to an extreme rainfall event with a 100-year return period in Hong Kong (DSD, 2018). Afterwards, an additional transient drying stage was conducted for 12 h using the same evaporative flux of 3.3×10^{-8} m/s to allow further development of water balance components.

In the parametric study, the transient seepage analysis is conducted by applying a rainfall event immediately after the initial steady-state seepage analysis. The same rainfall event as that in the validation run is applied to the top boundary AB. Similarly, an evaporative flux of 3.3×10^{-8} m/s is replaced at the top boundary to simulate the drying process after the 12-h rainfall event for further analysis of the water balance results. All other boundary conditions are the same as those in the transient drying stage in the validation run. Note that all results in the following sections are presented in terms of pore-water pressure instead of matric suction.

3. Results and discussion

3.1. Validation of the numerical model

Fig. 6a shows the comparison between the measured and computed pore-water pressure profiles at Section I–I during the rainfall infiltration test. Based on the numerical simulation, the computed results can match the experimental results well, except at the depth of 0.7 m. Such discrepancy at the depth of 0.7 m may be due to possible measurement error during the experiment. The fair consistency between the measured and computed pore-water pressure profiles demonstrates that the established numerical model is capable of simulating the pore water pressure changes in three-layer landfill cover system constructed with RCAs. Fig. 6b shows the comparison between the measured and computed water balance components. When compared with the measured water balance components, the computed surface runoff and change in soil water storage were overpredicted, while both the lateral diversions in FRC and CRC layers were underestimated. Regarding the surface runoff, the maximum difference between the measurements and simulations was about 53 mm at 24 h, which was approximately 12% of the total precipitation. The change in soil water storage was overpredicted since the middle of the rainfall event (6 h), with a difference of about 24 mm at 24 h. Consequently, less amount of lateral diversion in FRC and CRC layers was resulted

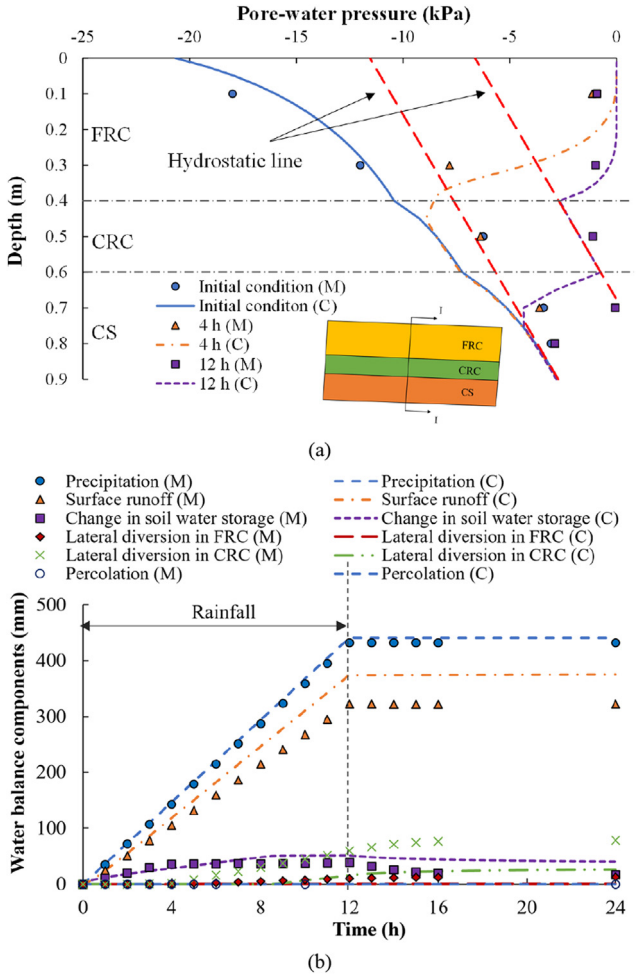

Fig. 6. Comparison between measured (M) and computed (a) pore-water pressure profiles at Section I–I and (b) water balance components (cumulative precipitation, surface runoff, change in soil water storage, lateral diversion and percolation).

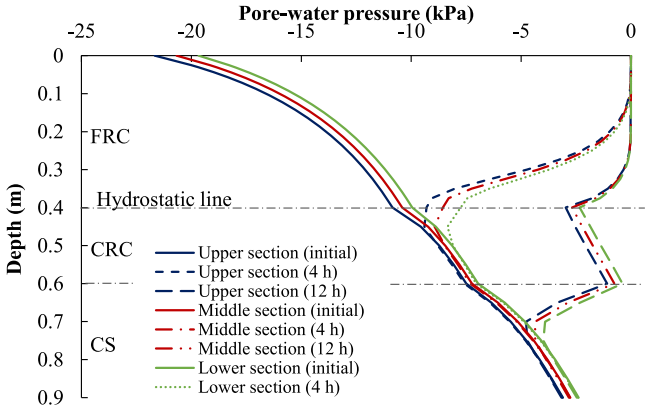

Fig. 7. Computed pore-water pressure distributions along the upper, middle and lower sections.

when compared with the measured values. The computed onset of the lateral diversion in CRC layer lagged behind as well. The total underestimated amount of lateral diversion in both layers at 24 h was about 65 mm, which was close to the sum of overestimation in surface runoff (53 mm) and change in soil water storage (24 mm).

The differences between the measurements and simulations may be because the effects of hydraulic hysteresis and the anisotropy of materials are ignored in the numerical simulations. Using the drying paths of WRCs, the amount of retained water at any given suction during rainfall is overestimated. Hence, the lateral diversion is underestimated. Despite the above discrepancies discussed, both the measured and computed results recorded no percolation throughout the 24 h rainfall duration. Furthermore, by comparing the computed pore-water pressure profiles at the upper (0.75 m), middle (1.50 m) and lower (2.25 m) sections along the flume model (Fig. 7), it is evident that they are very similar, implying that an infinite slope condition can be approximated. Therefore, the 3-m finite element model used in this study can approximately represent field-scale landfill cover.

3.2. Effects of particle size of the FRC and CRC layers

Fig. 8 shows the comparison of computed pore-water pressure profiles at Section I–I among the four runs in Series 1. Initially, the pore-water pressure profiles for each run (F0.05, F0.16, F0.5 and F1.6) were close to the hydrostatic line. After the 12-h rainfall event, the pore-water pressures in all runs increased especially in the top two layers. The wetting fronts reached a depth of about 0.8 m. In general, variations in particle size of the FRC layer had great influence on the pore-water pressure distributions in the FRC layer, but not in the CRC and CS layers. For F0.05 and F0.16, the FRC layer was close to saturation at the end of the rainfall. On the contrary, the pore-water pressures in the FRC layer remained negative for F0.5 and F1.6. This is attributed to the differences in the ratio between the k_s of FRC and rainfall intensity in each case (Ng and Shi, 1998). In F0.05 and F0.16, the k_s of FRC was smaller than or close to the rainfall intensity, hence the infiltrated water could not be drained away effectively from the layer. The pore-water pressures, therefore, built up gradually and approached zero. In contrast, the k_s values of FRC in F0.5 and F1.6 were higher than the rainfall intensity by at least one order of magnitude. This facilitated the drainage of water from the layer. Thus, the pore-water pressures in the FRC layer remained negative, or even approached a hydrostatic condition in F1.6. This is consistent with Yang et al. (2006) that the ratio between rainfall intensity and k_s plays an important role in affecting the pore-water pressure distribution in the top fine soil layer. Nevertheless, the pore water pressures in the CRC layer followed the hydrostatic line in all runs because of its high k_s. The pore-water pressures in the CS layer increased slowly due to the progressive seepage of water. Based on the computed results, it can be concluded that the CRC layer is sufficient to divert all the infiltrated water, regardless of the changes in particle size of the FRC layer. The pore-water pressure profiles also confirm that the 0.3 m thick CS layer has successfully impeded the seepage of water and prevented percolation.

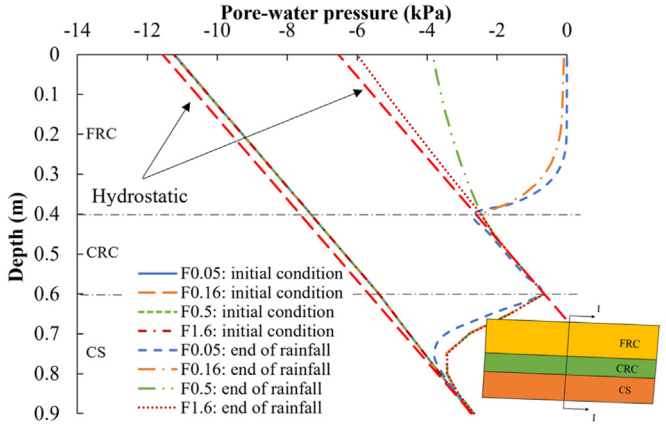

Fig. 8. Comparison of computed pore-water pressure profiles at Section I–I for runs with different D_{10} values of FRC.

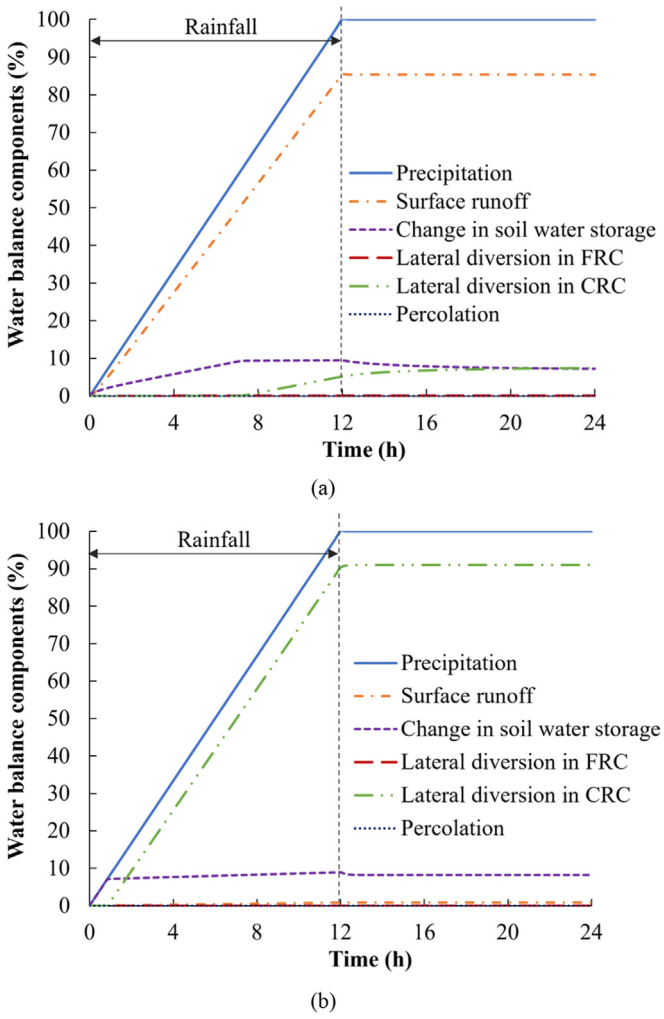

Fig. 9. Development of computed water balance components (cumulative precipitation, surface runoff, change in soil water storage, lateral diversion and percolation) with respect to the total precipitation for runs (a) F0.05 and (b) F1.6.

In order to further understand the influence of particle size of the FRC layer, water balance calculations from F0.05 and F1.6 are compared. These two cases are selected, as each of them represents the scenario where the k_s of FRC layer is smaller and larger than the rainfall intensity, respectively. Fig. 9a and b shows the computed water balance components with respect to the total precipitation for F0.05 and F1.6, respectively. In F0.05 (Fig. 9a), the surface runoff developed rapidly since the beginning of the rainfall event, while the increase in soil water storage was at a slower rate. This is because the k_s of the FRC layer was smaller than the rainfall intensity by one order of magnitude. Thus, a majority of the rainwater became surface runoff instead of infiltrating into the cover system. As the rainwater continued to infiltrate, the breakthrough of the capillary barrier occurred at around 7 h. Therefore, the soil water storage no longer increased and the lateral diversion in CRC layer began to take place at around 7 h. After 12 h, the rainfall stopped, but the lateral diversion in CRC layer continued to develop as the

stored water continued to discharge until the end of the simulation. No lateral diversion in FRC layer and percolation were observed during the 24 h period.

Interestingly, a different phenomenon can be observed in F1.6 (Fig. 9b). At the beginning of the rainfall, the increase in soil water storage was the same as the amount of precipitation, indicating that all the rainwater had infiltrated into the cover system. This is because the k_s of the FRC layer is significantly larger than the rainfall intensity. As a result, the capillary barrier effects disappeared quickly, and the infiltrated water reached the interface between the CRC and CS layers within the first hour. However, further downward migration of water was inhibited by the CS layer with low permeability by diverting the water along the CRC-CS interface. In this case, a majority of the rainwater was removed through the lateral diversion in CRC layer instead of surface runoff as in F0.05. After the rainfall stopped at 12 h, the soil water storage slightly decreased and no significant change in the water balance components was observed. No lateral diversion in FRC layer and bottom percolation were generated during the simulation. This is consistent with the results in F0.05. These results have illustrated that increasing the particle size of the FRC layer leads to a larger amount of infiltrated water and an earlier breakthrough of the capillary barrier. Therefore, to promote the performance of the three-layer cover system under extreme rainfall events, it is important that the CRC layer is sufficient to drain away the additional rainwater when large particle size is used in the FRC layer.

The water migration in the cover systems can be further interpreted by the water flow vectors. Fig. 10a and b shows the computed water flow vectors at the end of rainfall (12 h) for F0.05 and F1.6, respectively. When the D_{10} of FRC layer is 0.05 mm, water infiltration in the FRC layer was limited, which resulted in very small amount of lateral diversion in the CRC layer. However, for F1.6, a larger amount of rainwater infiltrated into the cover system due to the increased particle size of the FRC layer. Thus, it can be observed that the water flow vectors in the FRC layer in F1.6 (Fig. 10b) is more significant than that in F0.05 (Fig. 10a). Although breakthrough of the capillary barrier has already occurred at 12 h, the downward seepage of water in the CS layer was insignificant due to its low permeability. The infiltrated water was therefore removed through lateral diversion in the CRC layer as illustrated by the water flow vectors. Due to the increase in particle size, the infiltration rate in FRC layer increased from about 1×10^{-6} m/s to 1×10^{-5} m/s. Besides, the lateral flow velocity at the toe of CRC layer increased from about 1×10^{-4} m/s to 8×10^{-4} m/s. In contrast, the water flow in CS layer was much slower. The downward flow velocity of water in both runs was maintained in the order of 10^{-9} m/s. This demonstrates the effectiveness of the CS layer in impeding the downward seepage of water, ensuring the performance of the three-layer cover system when subjected to an extreme rainfall event. However, if ponding occurs in the CRC layer, the hydraulic gradient in the CS layer increases. As a result, the downward seepage of water in the layer speeds up, which can negatively affect the performance of the cover system.

Fig. 11 summarizes the influence of D_{10} value of FRC on the cumulative surface runoff, lateral diversion and percolation with respect to the total precipitation at 24 h. Lateral diversion in Fig. 11 refers to the total lateral diversion in both FRC and CRC layers. When the D_{10} value of FRC increased from 0.05 mm to 0.16 mm, the cumulative surface runoff decreased quickly from 85% to 1%, while the cumulative lateral diversion from the FRC and CRC layers increased from 7% to 91%. Such sharp changes were because of the increasing amount of rainwater infiltrated into the cover system and diverted through the CRC layer when a larger particle size of FRC was used. However, no further changes in these two components can be observed when the D_{10} value of FRC continued to increase. In all the runs, no percolation was generated regardless of the changes in particle size of the FRC layer. This implies that the particle size of the FRC layer does not have major influence on the performance of the three-layer landfill cover system under the extreme rainfall event.

Fig. 11 also shows the influence of D_{10} of CRC layer on cumulative surface runoff, lateral diversion and percolation with respect to the total precipitation at 24 h. It clearly shows that when D_{10} of CRC decreases from 10.7 mm to 3.4 mm (k_s from 2.5×10^{-1} m/s to 2.5×10^{-2} m/s), there are no changes in cumulative surface runoff, lateral diversion and percolation. It indicates that under the 100-year return period rainfall, the hydrological performance of the three-layer landfill cover is not sensitive to the particle size of the middle layer when D_{10} of CRC is larger than 3.4 mm. Therefore, based on the results shown in Fig. 11, it is recommended that the selection of particle size of FRC and CRC should be based on the availability of materials for constructing the cover system. Also, the presented results have indicated a possibility of simplifying the top two layers into one single layer. However, removing the top fine-

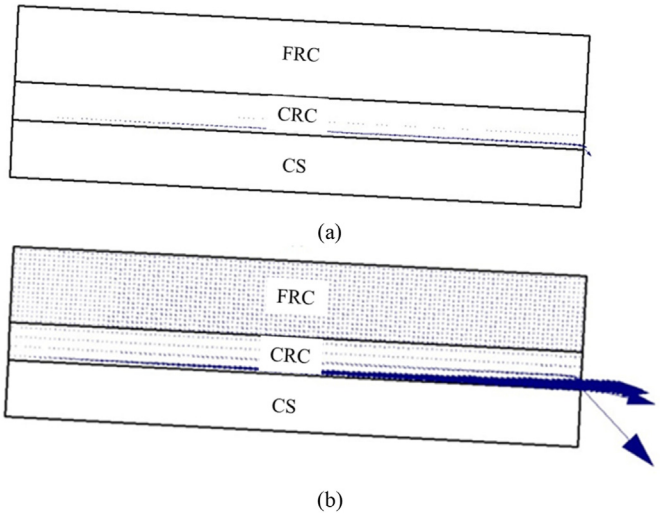

Fig. 10. Computed water flow vectors at the end of rainfall (12 h) for runs (a) F0.05 and (b) F1.6.

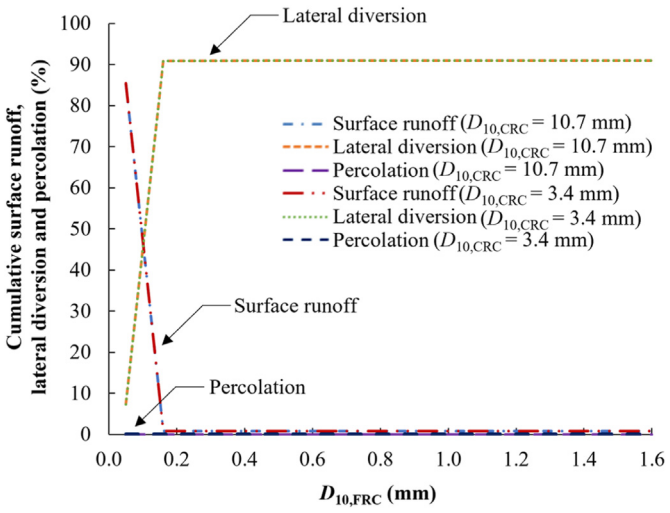

Fig. 11. Influence of D_{10} values of FRC and CRC on cumulative surface runoff, lateral diversion and percolation.

grained layer would potentially reduce the water storage capacity of the cover system. Therefore, further study is required to evaluate the feasibility of this approach.

3.3. Effects of particle size of the CS layer

Fig. 12 shows the comparison of computed pore-water pressure profiles at Section I–I among the three runs (i.e. CS0.002, CS0.006 and CS0.02). At the initial condition, the pore-water pressure profiles for CS0.006 and CS0.02 were approximately hydrostatic in contrast to CS0.002. This is because the permeabilities of the materials in these two runs are relatively large as compared to the applied rainfall intensity. After the 12-h rainfall event, the pore-water pressures for all three runs increased due to water infiltration. The pore-water pressure distributions at 12 h in the FRC and CRC layers for CS0.006 and CS0.02 were identical to CS0.002, which was close to the hydrostatic line. However, the wetting front in CS0.002 only reached a depth of about 0.8 m, while the wetting front in CS0.006 and CS0.02 reached the bottom of the cover system. The pore-water pressures at the bottom of the cover in these two runs increased to 0 kPa, resulting in water percolation. The results in Fig. 12 imply that the variation in particle size of the bottom layer does not affect the pore-water pressure distribution in the cover system if percolation has already occurred.

Fig. 13 summarizes the influence of D_{10} value of CS on cumulative lateral diversion and percolation with respect to the total precipitation at 24 h. According to the computed results in Fig. 13, the particle size of the bottom layer is important in controlling the amount of percolation from the cover system. When the D_{10} value of CS increased from 0.002 mm to 0.02 mm, the cumulative lateral diversion from the FRC and CRC layers slightly decreased from 91% to 87%, while the cumulative percolation increased from 0% to 5%. This is because the increased particle size of CS facilitates a faster downward seepage of water. Thus, a larger amount of water can percolate through the cover system after the breakthrough of the upper capillary barrier. Although water percolation occurred for CS0.006, the cumulative percolation at the end of the simulation (24 h) was less than 0.5% of the total precipitation. On the contrary, 5% of the total precipitation percolated through the cover system for CS0.02. However, this amount is still less than the 30 mm recommended design criterion suggested by USEPA (1993). As reported in previous studies, small rainfall events can be effectively prevented by CCBE (Khire et al., 2000; Albright et al., 2004; Rahardjo et al., 2016; Zhan et al., 2017). That means only heavy

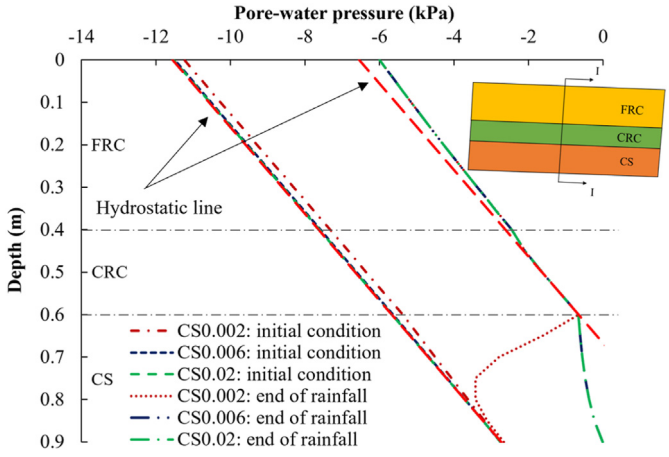

Fig. 12. Comparison of computed pore-water pressure profiles at Section I–I for runs with different D_{10} values of CS.

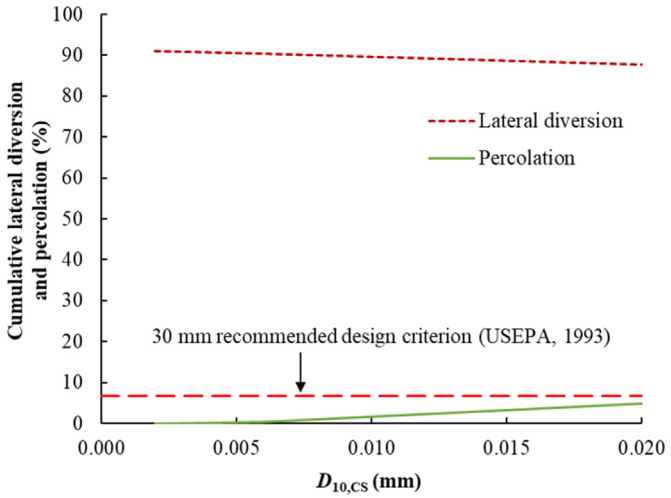

Fig. 13. Influence of D_{10} value of CS on cumulative lateral diversion and percolation.

rainfall would break through the capillary barrier and infiltrate into the bottom layer of three-layer landfill cover system, causing percolation. The percolation caused by the individual rainfall event is compared with the annual percolation limit of 30 mm suggested by USEPA (1993) if there is no other occurrence of rainfalls with a return period greater than 100 years within the same year.

The simulation durations of CS0.002, CS0.006 and CS0.02 were further extended until the completion of water percolation from the cover system. Fig. 14 shows the comparison of cumulative percolation between the three runs and other CCBEs. For CS0.02, the final amount of percolation is 29 mm, which is larger than those in other two-layer CCBE designs by Tami et al. (2004) and Zhan et al. (2017), but close to that in the three-layer CCBE design by Zhan et al. (2014). The percolation, however, is still smaller than the 30 mm design criterion suggested by USEPA (1993). This indicates the CS layer may not be effective in minimizing percolation when D_{10} is larger than 0.02 mm. On the contrary, if a smaller particle size (i.e. D_{10} value below 0.006 mm) is selected for the CS layer, the amount of percolation is considerably lower than the others. This implies that the particle size of the bottom CS layer plays an

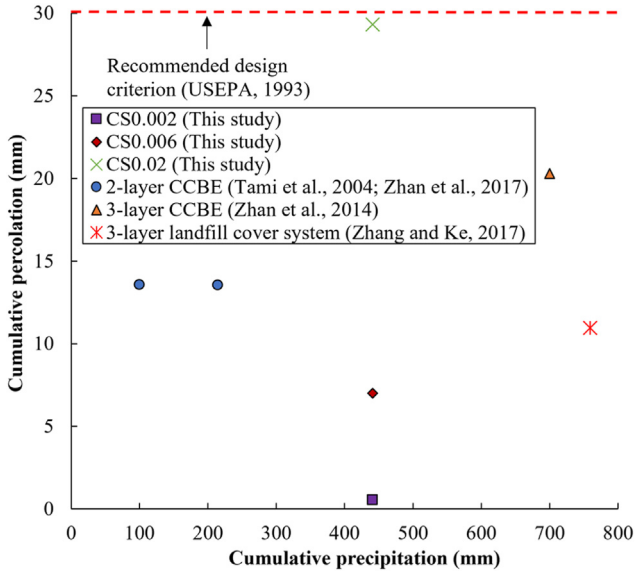

Fig. 14. Comparison of cumulative percolation for runs with different D_{10} values of CS and other CCBEs (2-layer CCBE (Tami et al., 2004; Zhan et al., 2017), 3-layer CCBE (Zhan et al., 2014), and 3-layer landfill cover system (Zhang and Ke, 2017)).

important role in affecting the performance of the three-layer landfill cover system under extreme rainfall event. In order to minimize water percolation effectively, a fine particle size with D_{10} smaller than 0.02 mm has to be selected for the CS layer. Although CS is used in the bottom layer in this study, it can be replaced by RCA and the obtained conclusions provide general guidance regarding the selection of particle size for RCAs. In both Figs. 13 and 14, the feasibility of implementing the proposed three-layer design with recycled concrete under humid climate has been demonstrated. It should be noted that according to the results reported by Ng et al. (2015a), the amount of percolation from the three-layer cover system increases with the duration of rainfall under the same return period. Therefore, rainfall with smaller intensity but longer duration would provide more conservative results in terms of percolation. Hence, the recommendations for practical design in this study are only applicable for the 100-year return period of rainfall condition with rainfall intensity larger than 36.8 mm/h.

4. Conclusions

A numerical study is conducted in this study to investigate the influence of particle size of RCAs on the performance of the three-layer landfill cover system without geomembrane. Different particle sizes, as characterized by the D_{10} value, are considered for the FRC (top), CRC (middle) and CS (bottom) layers. Pore-water pressure distributions and water balance components are analysed to evaluate the performance of the final cover. Before the numerical parametric study is carried out, the 2D numerical model is validated against a flume test.

Based on the parametric study, lateral diversion increases sharply when D_{10} of FRC increases from 0.05 mm to 0.16 mm, beyond which, there is no change in the lateral diversion. In general, the larger D_{10} of CRC (i.e. larger than 3.4 mm) does not have any influence on the cumulative surface runoff and lateral diversion. Regardless of the particle sizes of the FRC and CRC layers, water percolation can be successfully prevented by the bottom layer with low permeability and ponding does not occur in the CRC layer in all the runs. In addition, particle size induced changes in water retention capacity have negligible influence on the results. Thus, the selection of particle sizes of the FRC and CRC layers should be based on the availability of materials.

On the contrary, the particle size of the bottom layer has a determining influence on the performance of the three-layer landfill cover system. Increasing the particle size of the layer causes an earlier occurrence of water percolation in the cover system. When the D_{10} value of CS layer is larger than 0.02 mm, a significant amount of water percolation will occur. This study demonstrates that the alternative cover systems using RCAs for all the three layers can still perform well under the 100-year return period of rainfall in humid climates, provided that the bottom layer should have a D_{10} value not larger than 0.02 mm. Therefore, it is recommended that the bottom layer should have a D_{10} value smaller than 0.02 mm.

Declaration of competing interest

The authors declare that they have no known competing financial interests or personal relationships that could have appeared to influence the work reported in this paper.

Acknowledgments

The authors would like to thank the financial sponsorship from the National Natural Science Foundation of China (Grant Nos. U20A20320 and 51778166) and the funding from the State Key Laboratory of Subtropical Building Science in South China University of Technology (Grant No. 2022ZC01). The fifth author Mr. Qi Zhang is also grateful for the support of the Hong Kong PhD Fellowship Scheme (HKPFS) provided by the Research Grants Council of Hong Kong Special Administrative Region, China.

References

Agus, S.S., Leong, E.C., Rahardjo, H., 2005. Estimating permeability functions of Singapore residual soils. Eng. Geol. 78 (1–2), 119–133.
Albright, W.H., Benson, C.H., Gee, G.W., et al., 2006. Field performance of a compacted clay landfill final cover at a humid site. J. Geotech. Geoenviron. Eng. 132 (11), 1393–1403.
Albright, W.H., Benson, C.H., Gee, G.W., et al., 2004. Field water balance of landfill final covers. J. Environ. Qual. 33 (6), 2317–2332.
Amaya, P., Queen, B., Stark, T.D., Choi, H., 2006. Case history of liner veneer instability. Geosynth. Int. 13 (1), 36–46.
Artiola, J.F., Rasmussen, C., Freitas, R., 2012. Effects of a biochar-amended alkaline soil on the growth of romaine lettuce and bermudagrass. Soil Sci. 177 (9), 561–570.
ASTM D2434-68, 2006. Standard Test Method for Permeability of Granular Soils (Constant Head). ASTM International, West Conshohocken, PA, USA.
ASTM D2487-11, 2011. Standard Practice for Classification of Soils for Engineering Purposes (Unified Soil Classification System). ASTM International, West Conshohocken, PA, USA.
ASTM D5084-10, 2010. Standard Test Methods for Measurement of Hydraulic Conductivity of Saturated Porous Materials Using a Flexible Wall Permeameter. ASTM International, West Conshohocken, PA, USA.
ASTM D6836-16, 2016. Standard Test Methods for Determination of the Soil Water Characteristic Curve for Desorption Using Hanging Column, Pressure Extractor, Chilled Mirror Hygrometer, or Centrifuge. ASTM International, West Conshohocken, PA, USA.
Bardet, J.P., Jesmani, M., Jabbari, N., 2014. Permeability and compressibility of wax-coated sands. Geotechnique 64 (5), 341–350.
Chapuis, R.P., 2004. Predicting the saturated hydraulic conductivity of sand and gravel using effective diameter and void ratio. Can. Geotech. J. 41 (5), 787–795.
Chapuis, R.P., 2012. Predicting the saturated hydraulic conductivity of soils: a review. Bull. Eng. Geol. Environ. 71 (3), 401–434.
Chapuis, R.P., Aubertin, M., 2003. On the use of the Kozeny Carman equation to predict the hydraulic conductivity of soils. Can. Geotech. J. 40 (3), 616–628.
Chen, R., Liu, J., Ng, C.W.W., Chen, Z.K., 2019. Influence of slope angle on water flow in a three-layer capillary barrier soil cover under heavy rainfall. Soil Sci. Soc. Am. J. 83 (6), 1637–1647.
Cui, Y.F., Fang, F., Li, Y., Liu, H., 2022. Assessing effectiveness of a dual-barrier system for mitigating granular flow hazards through DEM-DNN framework. Eng. Geol. 306, 106742.
DSD, 2018. Stormwater Drainage Manual. Drainage Service Department (DSD), Hong Kong, China.
Dobson, M.C., Moffat, A.J., 1995. A re-evaluation of objections to tree planting on containment landfills. Waste Manag. Res. 13 (5), 579–600.
Evangelista, L., Brito, J. De, 2010. Durability performance of concrete made with fine recycled concrete aggregates. Cem. Concr. Compos. 32 (1), 9–14.
Fang, J., Cui, Y.F., Li, X., Nie, J., 2022. A new insight into the dynamic impact between geophysical flow and rigid barrier. Comput. Geotech. 148, 104790.
Fox, P.J., Thielmann, S.S., Stern, A.N., Athanassopoulos, C., 2014. Interface shear damage to a HDPE geomembrane. I: gravelly compacted clay liner. J. Geotech. Geoenviron. Eng. 140 (8), 04014039.
Fredlund, D.G., Xing, A., 1994. Equations for the soil water characteristic curve. Can. Geotech. J. 31 (4), 521–532.
Fredlund, M.D., Fredlund, D.G., Wilson, G.W., 2000. An equation to represent grain-size distribution. Can. Geotech. J. 37 (4), 817–827.
GarciaCalvo, J.L., Hidalgo, A., 2010. Development of low-pH cementitious materials for HLRW repositories: resistance against ground waters aggression. Cement Concr. Res. 40, 1290–1294.
Gabr, A.R., Cameron, D.A., 2012. Properties of recycled concrete aggregate for unbound pavement construction. J. Mater. Civ. Eng. 24 (6), 754–764.
GB 51220-2017, 2017. Technical Code for Municipal Solid Waste Sanitary Landfill Closure. Standardisation Administration of China, Beijing, China.
Hazen, A., 1911. Discussion of “Dams on sand foundations” by A.C. Koenig. Trans. Am. Soc. Civ. Eng. 73, 190–207.
Ju, S.H., Kung, K.J., 1997. Mass types, element orders and solution schemes for the Richards equation. Comput. Geosci. 23 (2), 175–187.
Khire, M.V., Benson, C.H., Bosscher, P.J., 2000. Capillary barriers: design variables and water balance. J. Geotech. Geoenviron. Eng. 126 (8), 695–708.
Lee, K.H., Yang, K.H., 2016. Development of a neutral cementitious material to promote vegetation concrete. Construct. Build. Mater. 127, 442–449.
Leong, E.C., Rahardjo, H., 1997. Review of soil-water characteristic curve equations. J. Geotech. Geoenviron. Eng. 123 (12), 1106–1117.
Li, X., Li, X., Wu, Y., Wu, L., Yue, Z., 2022. Selection criteria of mesh size and time step in FEM analysis of highly nonlinear unsaturated seepage process. Comput. Geotech. 146, 104712.
Li, Y., Satyanaga, A., Rahardjo, H., 2021. Characteristics of unsaturated soil slope covered with capillary barrier system and deep-rooted grass under different rainfall patterns. Int. Soil Water Conserv. Res. 9 (3), 405–418.

Lu, B.W., 2019. Water Infiltration into a Sustainable Three-Layer Landfill Cover System Using Recycled Concrete Aggregates. MSc Thesis. The Hong Kong University of Science and Technology, Hong Kong, China.
Marshall, T.J., 1958. A relation between permeability and size distribution of pores. J. Soil Sci. 9 (1), 1–8.
Mualem, Y., 1976. A new model for predicting the hydraulic conductivity of unsaturated porous media. Water Resour. Res. 12 (3), 513–522.
Ng, C.W.W., Chen, R., Coo, J.L., et al., 2019a. A novel vegetated three-layer landfill cover system using recycled construction wastes without geomembrane. Can. Geotech. J. 56 (12), 1863–1875.
Ng, C.W.W., Coo, J.L., Chen, Z.K., Chen, R., 2016. Water infiltration into a new three-layer landfill cover system. J. Environ. Eng. 142 (5), 04016007.
Ng, C.W.W., Guo, H.W., Ni, J.J., et al., 2022a. Long-term field performance of non-vegetated and vegetated three-layer landfill cover systems using construction waste without geomembrane. Géotechnique. https://doi.org/10.1680/jgeot.21.00238.
Ng, C.W.W., Guo, H.W., Ni, J.J., Zhang, Q., Chen, Z.K., 2022b. Effects of soil-plant-biochar interactions on water retention and slope stability under various rainfall patterns. Landslides 19, 1379–1390.
Ng, C.W.W., Liu, J., Chen, R., Coo, J.L., 2015a. Numerical parametric study of an alternative three-layer capillary barrier cover system. Environ. Earth Sci. 74 (5), 4419–4429.
Ng, C.W.W., Liu, J., Chen, R., Xu, J., 2015b. Physical and numerical modeling of an inclined three-layer (silt/gravelly sand/clay) capillary barrier cover system under extreme rainfall. Waste Manage. (Tucson, Ariz.) 38, 210–221.
Ng, C.W.W., Lu, B.W., Ni, J.J., Chen, Y.M., Chen, R., Guo, H.W., 2019b. Effects of vegetation type on water infiltration in a three-layer cover system using recycled concrete. J. Zhejiang Univ. - Sci. 20 (1), 1–9.
Ng, C.W.W., Menzies, B., 2007. Advanced Unsaturated Soil Mechanics and Engineering. Taylor & Francis Group.
Ng, C.W.W., Pang, Y.W., 2000. Influence of stress state on soil-water characteristics and slope stability. J. Geotech. Geoenviron. Eng. 126 (2), 157–166.
Ng, C.W.W., Shi, Q., 1998. A numerical investigation of the stability of unsaturated soil slopes subjected to transient seepage. Comput. Geotech. 22 (1), 1–28.
Nwakaire, C.M., Yap, S.P., Onn, C.C., Yuen, C.W., Ibrahim, H.A., 2020. Utilisation of recycled concrete aggregates for sustainable highway pavement applications; a review. Construct. Build. Mater. 235, 117444.
Oikonomou, N.D., 2005. Recycled concrete aggregates. Cem. Concr. Compos. 27 (2), 315–318.
Qian, X., Koerner, R.M., Gray, D.H., 2001. Geotechnical Aspects of Landfill Construction and Design. Prentice Hall, Inc., Englewood Cliffs, NJ, USA.
Rahardjo, H., Krisdani, H., Leong, E.C., 2007. Application of unsaturated soil mechanics in capillary barrier system. In: Proceedings of the 3rd Asian Conference on Unsaturated Soils, pp. 127–137, 2007.
Rahardjo, H., Satyanaga, A., Harnas, F.R., Leong, E.C., 2016. Use of dual capillary barrier as cover system for a sanitary landfill in Singapore. Indian Geotech. J. 46 (3), 228–238.
Rahardjo, H., Satyanaga, A., Leong, E.C., Wang, J.Y., 2013a. Unsaturated properties of recycled concrete aggregate and reclaimed asphalt pavement. Eng. Geol. 161, 44–54.
Rahardjo, H., Santoso, V.A., Leong, E.C., Ng, Y.S., Tam, C.P.H., Satyanaga, A., 2013b. Use of recycled crushed concrete and Secudrain in capillary barriers for slope stabilization. Can. Geotech. J. 50 (6), 662–673.
Ross, B., 1990. The diversion capacity of capillary barriers. Water Resour. Res. 26 (10), 2625–2629.
Sezer, A., Göktepe, A.B., Altun, S., Bassiliades, N., 2009. Estimation of the permeability of granular soils using neuro-fuzzy system. In: AIAI-2009 Workshops Proceedings, pp. 333–342.
Smesrud, J.K., Selker, J.S., 2001. Effect of soil-particle size contrast on capillary barrier performance. J. Geotech. Geoenviron. Eng. 127 (10), 885–888.
Tabsh, S.W., Abdelfatah, A.S., 2009. Influence of recycled concrete aggregates on strength properties of concrete. Construct. Build. Mater. 23 (2), 1163–1167.
Tami, D., Rahardjo, H., Leong, E.C., Fredlund, D.G., 2004. A physical model for sloping capillary barriers. Geotech. Test J. 27 (2), 173–183.
Taylor, D.W., 1948. Fundamentals of Soil Mechanics. John Wiley & Sons, Inc.
USEPA, 1993. Solid Waste Disposal Facility Criteria: Technical Manual. Technical Report No. EPA530-R-93-017. Environmental Protection Agency, Washington D.C., USA.
van Genuchten, M.T., 1980. A closed-form equation for predicting the hydraulic conductivity of unsaturated soils. Soil Sci. Soc. Am. J. 44 (5), 892–898.
Vereecken, H., Schnepf, A., Hopmans, J.W., et al., 2016. Modeling soil processes: review, key challenges, and new perspectives. Vadose Zone J. 15 (5), 1–57.
Vogel, H.J., Ippisch, O., 2008. Estimation of a critical spatial discretization limit for solving Richards' equation at large scales. Vadose Zone J. 7 (1), 112–114.
Wong, C.T., Leung, M.K., Wong, M.K., Tang, W.C., 2013. Afteruse development of former landfill sites in Hong Kong. J. Rock Mech. Geotech. Eng. 5 (6), 443–451.
Yang, H., Rahardjo, H., Leong, E.C., 2006. Behavior of unsaturated layered soil columns during infiltration. J. Hydrol. Eng. 11 (4), 329–337.
Yao, Y., Li, J., Ni, J.J., Liang, C., Zhang, A., 2022. Effects of gravel content and shape on shear behaviour of soil-rock mixture: experiment and DEM modelling. Comput. Geotech. 141, 104476.
Yao, Y., Ni, J.J., Li, J., 2021. Stress-dependent water retention of granite residual soil and its implications for ground settlement. Comput. Geotech. 129, 103835.
Zhan, L.T., Li, G.Y., Jiao, W.G., Wu, T., Lan, J.W., Chen, Y.M., 2017. Field measurements of water storage capacity in a loess–gravel capillary barrier cover using rainfall simulation tests. Can. Geotech. J. 54 (11), 1523–1536.
Zhan, T.L.T., Li, H., Jia, G.W., Chen, Y.M., Fredlund, D.G., 2014. Physical and numerical study of lateral diversion by three-layer inclined capillary barrier covers under humid climatic conditions. Can. Geotech. J. 51 (12), 1438–1448.
Zhang, L.M., Ke, Y.Q., 2017. Combinations of soil materials for granular capillary barriers for minimizing rainfall infiltration and gas emission. Can. Geotech. J. 54 (11), 1580–1591.
Zhang, W., Sun, C., 2014. Parametric analyses of evapotranspiration landfill covers in humid regions. J. Rock Mech. Geotech. Eng. 6 (4), 356–365.
Zhao, M., Jia, Y., Yuan, L., Qiu, J., Xie, C., 2019. Experimental study on the vegetation characteristics of biochar modified vegetation concrete. Construct. Build. Mater. 206, 321–328.

Prof. Charles Wang Wai Ng earned his PhD degree from the University of Bristol, UK in 1993. After carrying out post-doctoral research at the University of Cambridge between 1993 and 1995, he returned to Hong Kong, joined HKUST as Assistant Professor in 1995 and rose through the ranks to become Chair Professor in 2011. As a world authority on unsaturated soil mechanics, eco-geotechnical engineering and landslides, Prof. Ng is the Fellow of the Royal Academy of Engineering, immediate Past President of the International Society for Soil Mechanics and Geotechnical Engineering (2017–2022), Changjiang Scholar (Chair Professorship in Geotechnical Engineering), Fellow of the Hong Kong Academy of Engineering Sciences, and Overseas Fellow of Churchill College, the University of Cambridge. He is also the Fellow of the Institution of Civil Engineers, the American Society of Civil Engineers, and the Hong Kong Institution of Engineers. Currently, he is a co-Editor-in-Chief of the *Canadian Geotechnical Journal*. Prof. Ng has supervised more than 60 PhD and 60 MPhil students to graduation, published 390 SCI journal articles and 250 conference papers and delivered more than 100 keynotes and state-of-the-art reports across the six continents. He is the main author of three reference books: (i) A Short Course in Soil-structure Engineering of Deep Foundations, Excavations and Tunnels by Thomas Telford in 2004, (ii) Advanced Unsaturated Soil Mechanics and Engineering, and (iii) Plant-Soil Slope Interaction by CRC Press in 2007 and 2019, respectively.